Liquid Crystals

Synthesis and characterization of halogen-containing ferroelectric liquid crystals and side chain liquid crystalline polymers

Ging-Ho Hsiue [a] , Yi-An Sha [a] , Shih-Jung Hsieh [a c] , Ru-Jong Jeng [b] & Wen-Jang Kuo [a]

[a] Department of Chemical Engineering, National Tsing Hua University, Hsinchu, Taiwan 300, ROC

[b] Institute of Applied Chemistry, National Chiao Tung University, Hsinchu, Taiwan 300, ROC

[c] Department of Chemical Engineering, National Chung Hsing University, Taichung, Taiwan 402, ROC
Published online: 06 Aug 2010.

PLEASE SCROLL DOWN FOR ARTICLE

Synthesis and characterization of halogen-containing ferroelectric liquid crystals and side chain liquid crystalline polymers

GING-HO HSIUE*, YI-AN SHA, SHIH-JUNG HSIEH†, RU-JONG JENG‡
and WEN-JANG KUO

Department of Chemical Engineering, National Tsing Hua University, Hsinchu,
Taiwan 300, ROC
†Institute of Applied Chemistry, National Chiao Tung University, Hsinchu,
Taiwan 300, ROC
‡Department of Chemical Engineering, National Chung Hsing University,
Taichung, Taiwan 402, ROC

A new series of ferroelectric liquid crystals and side chain liquid crystalline polymers based on halogen-containing chiral centres has been synthesized. Chemical structures were analysed by NMR. Liquid crystal phases were characterized by differential scanning calorimetry, optical polarizing microscopy, and X-ray diffractometry. The behaviour of the liquid crystalline phases was investigated as a function of spacer units and differing terminal asymmetric moieties. It was found that phase transition temperatures decreased with increasing length of the oligooxyethylene spacer unit. Differing terminal asymmetric moieties led to differing mesophase phenomena. Furthermore, a wide temperature range (including room temperature) of a chiral smectic C phase was achieved.
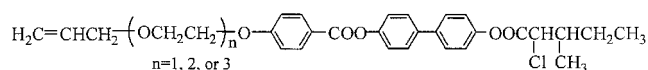
1. Introduction

During the past decade, ferroelectric liquid crystals (FLCs) have been extensively studied because of their fast response time and memory effect toward an applied electric field [1–6]. These characteristics make them suitable for electro-optical applications. Prompted by the development of surface stabilized ferroelectric liquid crystal (SSFLC) display technology [7], FLC materials and SSFLC cells have been vigorously investigated [8].

For display use, FLC materials have mostly been designed to provide a wide temperature range of the FLC phase, including room temperature [9], and a large value of the spontaneous polarization (P_s). These properties are influenced by the design of the molecular structures of FLC mesogens. The fundamental molecular structure of an FLC includes a mesogenic group, a spacer chain unit, and a chiral centre unit (terminal chain units). The mesogenic group often consists of at least two linked rigid groups with lateral substituents [10]. The length and chemical structure of the spacer unit appear to be important factors in LFC phase formation and temperature range. The oxyethylene group as spacer

unit favours a reduction in the phase transition temperatures. As the number of oxyethylene units increases, the transition temperature decreases [11]. The chiral centre is usually the major part of the terminal chain because the P_s value is affected by the asymmetric atom and its position, and the length of the terminal chain unit. In addition, incorporation of a polar group (F, Cl, Br, CN, CF$_3$, etc.) onto the chiral centre close to the core can maximize the P_s value [12, 13].

In our previous work, a series of chlorine-containing FLCs was synthesized and characterized [14]. These monomers have a wide temperature range of the chiral smectic C phase—including room temperature; their chemical structures are shown below:

$$H_2C=CHCH_2\!-\!\left(OCH_2CH_2\right)_n\!\!-\!O\!-\!\!\bigcirc\!\!-COO\!-\!\!\bigcirc\!\!-\!\!\bigcirc\!\!-OOCCHCHCH_2CH_3$$
n=1, 2, or 3   Cl CH$_3$

In this paper, a new series of ferroelectric liquid crystals and side chain liquid crystalline polymers is reported. These liquid crystalline materials consist of various halogen-containing chiral moieties (F, Cl, and Br), oligooxyethylene spacers, and ester core units. The influences of the varied halogen-containing chiral tails and spacer units on mesophase formation are also discussed.

*Author for correspondence; e-mail: ghhsiue@che.nthu.edu.tw

2. Experimental

2.1. *Materials*

Allyl bromide, 2-chloroethanol, 2-(2-chloroethoxy)-ethanol, 2-[2-(2-chloroethoxy)ethoxy]ethanol, hydrogen fluoride–pyridine, trifluoromethanesulfonic anhydride, tetrabutylammonium fluoride hydrate, and hydrogen hexachloroplatinate(IV) hydrate were purchased from Adrich Chemical Co. 4,4′-Dihydroxybiphenyl, *N,N*′-dicyclohexylcarbodiimide (DCC), 4,4′-biphenol, L-isoleucine, sodium nitrite, and pyridine were purchased from Tokyo Chemical Industry Co. Ltd. 4-Dimethylamino-pyridine (DMAP) and benzophenone were purchased from Lancaster Chemicals Ltd; poly(methylhydrogen-siloxane) ($[\eta] = 30$) was purchased from United Chemical Technologies, Inc; hexane, ethyl acetate, dichloromethane, acetonitrile, and methanol were purchased from TEDIA. All these chemicals were used as received. Tetrahydro-furan and toluene purchased from TEDIA were distilled over sodium using benzophenone as indicator under a nitrogen atmosphere.

2.2. *Characterization methods*

^{1}H NMR and ^{19}F NMR spectra were obtained on Bruker AM-400 NMR or Jeol JNM-FX100 spectro-meters. Transition temperatures were determined as the maxima of endothermic or exothermic peaks using a Seiko SSC 5200 differential scanning calorimeter (DSC); heating and cooling rates were 10°C min^{-1}. The transition temperatures were specifically obtained from the first heating and second cooling scans. A Nikon Micro-photo-Fx polarizing optical microscope (POM) equipped with a Mettler FP82 hot stage was used to observe the thermal transitions and anisotropic textures. X-ray diffraction (XRD) measurements were performed with a Rigaku R-axis IIC powder diffractometer. A mono-chromatized X-ray beam from nickel-filtered CuK$_\alpha$ radiation with a wavelength of 0.15406 nm was used. A thermal controller was added to the X-ray system for thermal measurement with a tolerance of ± 0.5°C.

2.3. *Synthesis of monomers*

The syntheses of the liquid crystalline monomers are outlined in schemes 1–3.

2.3.1. *4-(2-Allyloxyethoxy)benzoic acid (S-1); 4-[2-(2-allyloxyethoxy)ethoxy]benzoic acid (S-2); 4-{2-[2-(2-allyloxyethoxy)ethoxy]ethoxy}benzoic acid (S-3)*

The syntheses of these compounds via esterification and etherification reactions have been reported previously [14].

2.3.2. *(2S,3S)-2-Fluoro-3-methylpentanoic acid (Fs-1)*

In a 500 ml round-bottom flask, hydrogen fluoride-pyridine (100 g) was added dropwise to pyridine (60 ml) under N$_2$ at 0°C; after 10 min, L-isoleucine (7.87 g, 60 mmol) was added to the reaction mixture. Sodium nitrite powder (6.21 g, 90 mmol) was then added under
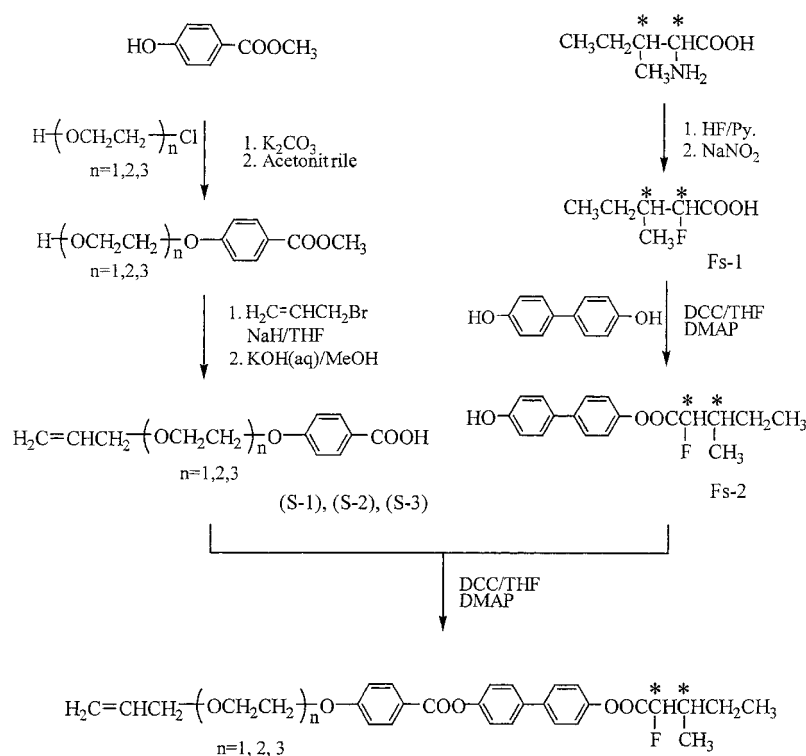
Scheme 1. Synthesis of monomers MD*n*12Fs (*n* = 1, 2, 3).
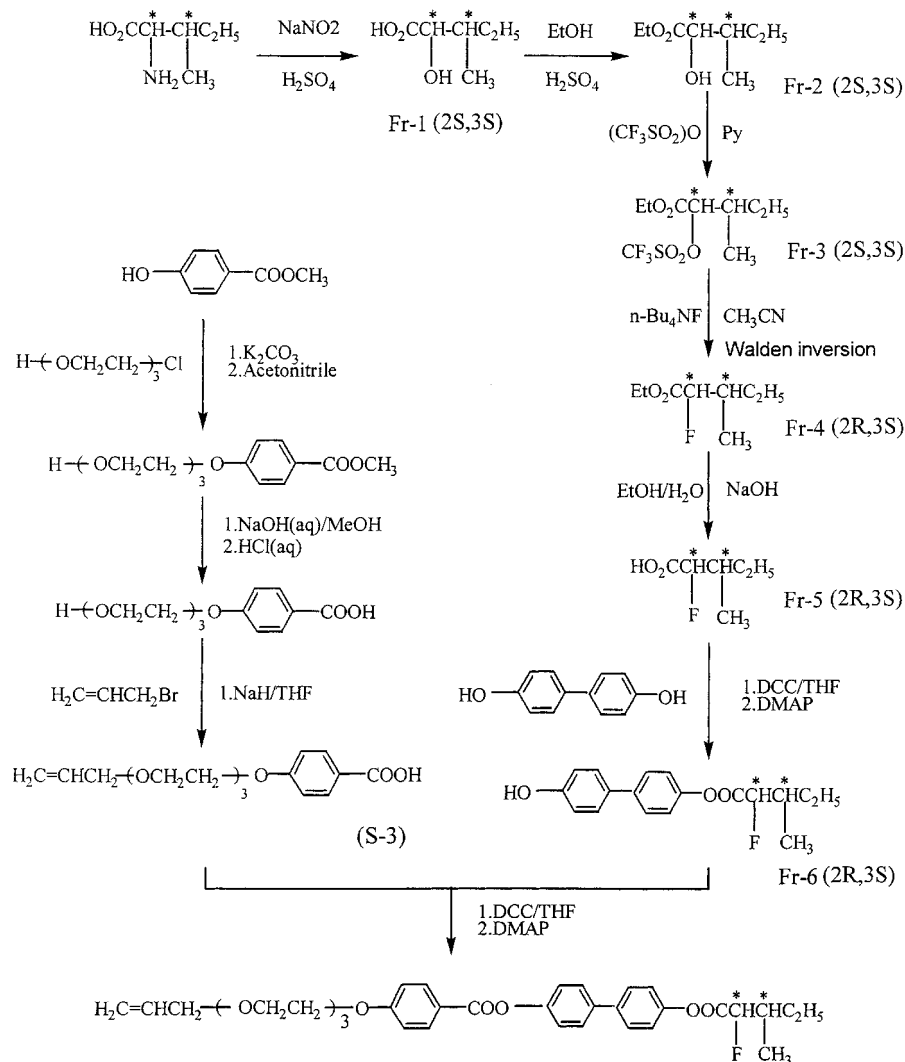
Scheme 2. Synthesis of monomer MD312Fr.

N$_2$ at 0°C. After stirring the reaction mixture for 5 h, cooling was removed, and the mixture held at room temperature for 24 h. The reaction mixture was then added to 500 ml of water and the mixture was extracted with ethyl ether. The organic phase solvent was evaporated and a colourless oily product was finally obtained after distillation (78–80°C, 4 mm Hg); yield 27.6%. ^{1}H NMR (DMSO-d$_6$): δ = 0.97 (t, 3H, C$\underline{H}_3$–CH$_2$–), 1.12 (d, 3H, –CH(C$\underline{H}_3$)–), 1.44 and 1.63 (m, 2H, CH$_3$C$\underline{H}_2$–), 2.17 (m, 1H, –C$\underline{H}$(CH$_3$)–), 4.93 (d, 1H, –C$\underline{H}$(F)–). ^{19}F NMR (DMSO-d$_6$): δ = – 243.42 (s, –CH($\underline{F}$)).

### 2.3.3. *(2S,3S)-2-Hydroxy-3-methylpentanoic acid (Fr-1)*

L-isoleucine (49.5 g, 377 mmol) was added to 2.67M H$_2$SO$_4$ aqueous solution (586 ml) at 0°C under N$_2$. Sodium nitrite (39.4 g, 570 mmol) dissolved in water (150 ml) was added dropwise under N$_2$ at 0°C and the mixture stirred at room temperature overnight. The reaction mixture was then extracted with ethyl ether;

after evaporating the solvent, a dark yellow oily product was obtained; yield 80%. ^{1}H NMR (DMSO-d$_6$): δ = 0.84 (t, 3H, –CH$_2$–C$\underline{H}_3$), 0.87 (d, 3H, –CH(C$\underline{H}_3$)–), 1.02–1.29 and 1.29–1.53 (m, 2H, –C$\underline{H}_2$CH$_3$), 1.53–1.57 (m, 1H, –C$\underline{H}$CH$_2$), 3.79 (m, 1H, –C$\underline{H}$(OH)–).

2.3.4. *Ethyl (2S,3S)-2-hydroxy-3-methylpentanoate (Fr-2)*

A mixture of 39.5 g (299 mmol) of Fr-1, 7.5 ml of H$_2$SO$_4$ and 300 ml of anhydrous ethanol was stirred under reflux for 24 h; ethanol was then distilled off. The reaction mixture was extracted with ethyl ether after saturated with an aqueous solution of NaHCO$_3$. The organic phase solvent was evaporated off, and a colourless oily product obtained by distillation (62–65°C, 6 mm Hg). ^{1}H NMR (DMSO-d$_6$): δ = 0.91 (t, 3H, –CH$_2$C$\underline{H}_3$), 0.99 (d, 3H, –CHC$\underline{H}_3$–C$_2$H$_5$), 1.13–1.53 (m, 2H, –C$\underline{H}_2$CH$_3$), 1.31 (t, 3H, –COOCH$_2$C$\underline{H}_3$),
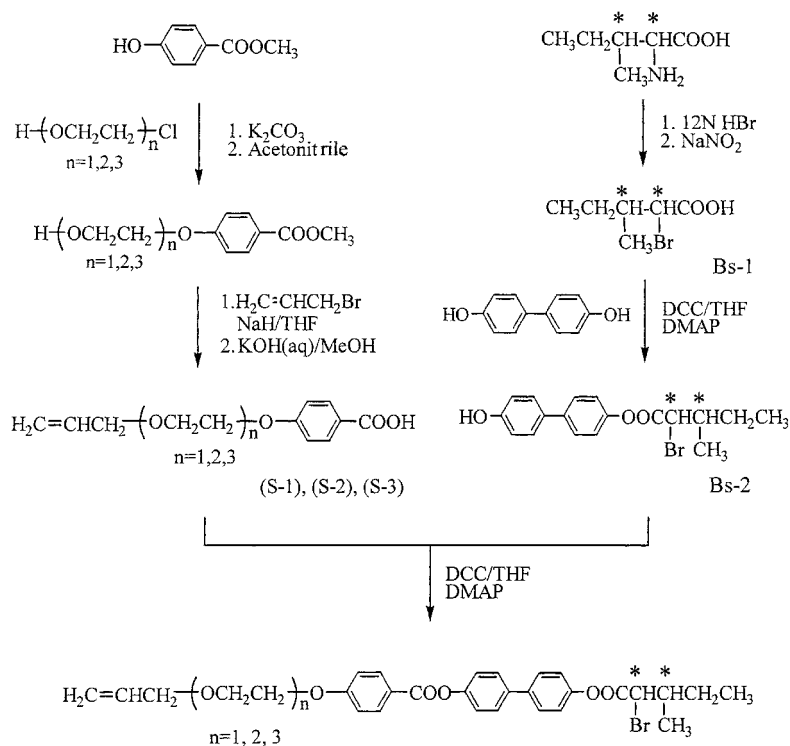
Scheme 3. Synthesis of monomers MD*n*12Bs (*n* = 1, 2, 3).

1.73–1.93 (m, 1H, −C$\underline{H}$(CH$_3$)−), 2.78 (br, s, 1H, −CH(O$\underline{H}$)−), 4.08 (d, 1H, −C$\underline{H}$(OH)−), 4.26 (q, 2H, −COOC$\underline{H}_2$CH$_3$).

2.3.5. *Ethyl (2S,3S)-2-(trifluoromethyl)sulfonyloxy-3-methylpentanoate (Fr-3)*

In a 500 ml polyproplene reactor, 34.5 g (325 mmol) of Fr-2, 200 ml of anhydrous dichloromethane and 18.6 ml of anhydrous pyridine was stirred under N$_2$ at 0°C. Trifluoromethylsulfonic anhydride (50 g, 177 mmol) was added dropwise. After 2 h the reaction mixture was added to 500 ml of water and the mixture extracted twice with dichloromethane. The organic phase was extracted with a 10 wt % aqueous solution of HCl, and the solvent evaporated to yield a colourless product after distillation (55–61°C, 0.4 mm Hg); yield 85.4%. ^{1}H NMR (DMSO-d$_6$): δ = 0.95 (t, 3H, −CH$_2$C$\underline{H}_3$), 1.07 (d, 3H, −CHC$\underline{H}_3$−C$_2$H$_5$), 1.19–1.64 (m, 2H, −C$\underline{H}_2$CH$_3$), 1.33 (t, 3H, −COOCH$_2$C$\underline{H}_3$), 2.05–2.27 (m, 1H, −C$\underline{H}$CH$_3$−), 4.31 (q, 2H, −COOC$\underline{H}_2$CH$_3$), 5.01 (d, 1H, −C$\underline{H}$(OSO$_2$CF$_3$)−).

2.3.6. *Ethyl (2R,3S)-2-fluoro-3-methylpentanoate (Fr-4)*

A solution of tetrabutylammonium fluoride hydrate (40 g) in 150 ml acetonitrile was added dropwise to a solution of Fr-3 (36.7 g, 133 mmol) in 150 ml acetonitrile at 80°C under N$_2$. After stirring the reaction mixture under reflux for 3 h, the acetonitrile was distilled off. The crude product was purified by flash chromato-graphy on silica gel with ethyl acetate and hexane as eluant. A colourless product was obtained by distillation (59–63°C, 9 mm Hg); yield 81.9%. ^{1}H NMR (DMSO-d$_6$): δ = 0.95 (t, 3H, −CH$_2$C$\underline{H}_3$), 0.96 (d, 3H, −CHC$\underline{H}_3$−C$_2$H$_5$), 1.19–1.65 (m, 2H, −C$\underline{H}_2$CH$_3$), 1.32 (t, 3H, −COOCH$_2$C$\underline{H}_3$), 1.75–2.12 (m, 1H, −C$\underline{H}$CH$_3$−), 4.28 (q, 2H, −COOC$\underline{H}_2$CH$_3$), 5.01 (d, 1H, −C$\underline{H}$F−). ^{19}F NMR (DMSO-d$_6$): δ = − 251.26 (−CH$\underline{F}$−).

2.3.7. *(2R,3S)-2-Fluoro-3-methylpentanoic acid (Fr-5)*

A mixture of 16.7 g (103 mmol) of Fr-4, 6 ml of 50 wt % aqueous sodium hydroxide, 20 ml of ethanol, and 200 ml of water was stirred under reflux for 24 h; ethanol was then distilled off. After cooling at 0°C, the reaction mixture was acidified with 5N hydrochloric acid and extracted with ethyl acetate. The organic phase solvent was evaporated off, and a colourless oily product obtained by distillation (78–80°C, 4 mm Hg); yield 76%. ^{1}H NMR (DMSO-d$_6$): δ = 0.89 (t, 3H, C$\underline{H}_3$CH$_2$−), 0.97 (d, 3H, −CH(C$\underline{H}_3$)−), 1.06–1.32, 1.32–1.56 (m, 2H, CH$_3$C$\underline{H}_2$−), 1.71–2.13 (m, 1H, −C$\underline{H}$(CH$_3$)−), 5.01 (d, 1H, −C$\underline{H}$F−). ^{19}F NMR (DMSO-d$_6$): δ = − 251.26 (−CH($\underline{F}$)−).

2.3.8. *(2S,3S)-2-Bromo-3-methylpentanoic acid (Bs-1)*

L-isoleucine (7.9 g, 60 mmol) and 75 ml 6N HBr were placed in a 500 ml round-bottom flask equipped with a magnetic stirrer at 0°C. Sodium nitrite (6.21 g, 90 mmol)

aqueous solution was added dropwise below 5°C under N_2. After stirring the reaction mixture for 5 h, cooling was removed, and the mixture held at room temperature for 24 h; it was then extracted with ethyl ether. The organic phase solvent was evaporated, and a red oily product obtained by distillation (140°C, 20 mm Hg); yield 73%. ^{1}H NMR (DMSO-d_6): $\delta = 0.96$ (t, 3H, −CH$_2$C$\underline{H}_3$), 1.13 (d, 3H, −CHC$\underline{H}_3$−), 1.39 and 1.83 (m, 2H, −C$\underline{H}_2$CH$_3$), 2.18 (m, 1H, −C$\underline{H}$CH$_3$), 4.09 (d, 1H, −C$\underline{H}$Br−), 11.8 (br, −COO$\underline{H}$).

2.3.9. *4,4′-Dihydroxybiphenyl (2S,3S)-2-fluoro-3-methyl-pentanoate (Fs-2); 4,4′-dihydroxybiphenyl (2R,3S)-2-fluoro-3-methylpentanoate (Fr-6); 4,4′-dihydroxybiphenyl (2S,3S)-2-bromo-3-methylpentanoate (Bs-2)*

These compounds were synthesized by similar methods. As an example, the synthesis of 4,4′-dihydroxy-biphenyl (2S,3S)-3-fluoro-3-methylpentanoate (Fs-2) is described as follows. In a 100 ml round-bottom flask, (2S,3S)-2-fluoro-3-methylpentanoic acid (3 g, 22.3 mmol), 4,4′-dihydroxybiphenyl (11 g, 59 mmol), dimethylamino-pyridine (0.5 g, 4 mmol), *N,N′*-dicyclohexylcarbodiimide (4.1 g, 20 mmol), and dried THF (50 ml) were stirred under N_2 at 0°C overnight. The solution was filtered and the filtrate evaporated. The product was purified by chromatography on silica gel with ethyl acetate and hexane as eluant. Yield (Fs-2) 70.5%, (Fr-6) 69.7,

(Bs-2) 75.5. (*Fs-2*) ^{1}H NMR (CDCl3): $\delta = 0.97$ (t, 3H, C$\underline{H}_3$CH$_2$−), 1.12 (d, 3H, −CH(C$\underline{H}_3$)−), 1.44 and 1.63 (m, 2H, CH$_3$C$\underline{H}_2$−), 2.17 (m, 1H, −C$\underline{H}$(CH$_3$)−), 4.93 (d, 1H, −C$\underline{H}$F−), 6.89, 7.15, 7.42 and 7.52 (4d, 8H, aromatic protons); ^{19}F NMR (CDCl3): $\delta = -243.42$ (−CH$\underline{F}$−). (*Fr-6*) ^{1}H NMR (CDCl3): $\delta = 0.97$ (t, 3H, C$\underline{H}_3$CH$_2$−), 1.12 (d, 3H, −CH(C$\underline{H}_3$)−), 1.44 and 1.63 (m, 2H, CH$_3$C$\underline{H}_2$−), 2.17 (m, 1H, −C$\underline{H}$(CH$_3$)−), 5.05 (d, 1H, −C$\underline{H}$F−), 6.87, 7.12, 7.39 and 7.52 (4d, 8H, aromatic protons); ^{19}F NMR (CDCl3): $\delta = -251.26$ (−CH$\underline{F}$−). (*Bs-2*) ^{1}H NMR (CDCl3): $\delta = 0.96$ (t, 3H, −CH$_2$C$\underline{H}_3$), 1.13 (d, 3H, −CHC$\underline{H}_3$−), 1.39 and 1.83 (m, 2H, −C$\underline{H}_2$CH$_3$), 2.18 (m, 1H, −C$\underline{H}$CH$_3$), 4.09 (d, 1H, −C$\underline{H}$Br−), 6.89, 7.15, 7.42 and 7.52 (4d, 8H, aromatic protons).

2.3.10. *Synthesis of FLC monomers MDn12Fs, MDn12Fr, and MDn12Bs*

These products were synthesized, respectively, in the same manner as compounds Fs-2, Fr-6, or Bs-2; ^{1}H NMR spectra are listed in table 1.

MDn12Fs stands for the following series: 4′-[(2S,3S)-2-fluoro-3-methylpentanoyloxy]-4-biphenyl 4-(2-allyloxy-ethoxy)benzoate (MD112Fs); 4′-[(2S,3S)-2-fluoro-3-methylpentanoyloxy]-4-biphenyl 4-[2-(2-allyl-oxyethoxy)-ethoxy]benzoate (MD212Fs); 4′-[(2S,3S)-2-fluoro-3-methylpentanoyloxy]-4-biphenyl 4-{2-[2-(2-allyloxy-ethoxy)ethoxy]ethoxy}benzoate (MD312Fs).

Table 1. Chemical shift and optical rotation values of compounds MD*n*12Fs, MD312Fr and MD*n*12Bs.

Compound	$[\alpha]_d^{25\,a}$	NMR spectra[b]
MD112Fs	− 9.789	^{1}H NMR: 0.97 (t, 3H, C$\underline{H}_3$CH$_2$−), 1.12 (d, 3H, −CH(C$\underline{H}_3$)−), 1.44 and 1.63 (m, 2H, CH$_3$C$\underline{H}_2$−), 2.17 (m, 1H, −C$\underline{H}$(CH$_3$)−), 4.93 (dd, 1H, −C$\underline{H}$F−), 3.81–4.20 (m, 6H, −C$\underline{H}_2$−(OC$\underline{H}_2$C$\underline{H}_2$)−), 5.23 and 5.9 (m, 3H, C$\underline{H}_2$=C$\underline{H}$−), 6.9–8.15 (6d, 12 aromatic protons). ^{19}F NMR: − 243.42 (−CH$\underline{F}$−).
MD212Fs	− 8.366	^{1}H NMR: 0.98 (t, 3H, C$\underline{H}_3$CH$_2$−), 1.12 (d, 3H, −CH(C$\underline{H}_3$)−), 1.44 and 1.65 (m, 2H, CH$_3$C$\underline{H}_2$−), 2.17 (m, 1H, −C$\underline{H}$(CH$_3$)−), 4.93 (dd, 1H, −C$\underline{H}$F−), 3.61–4.22 (m, 10H, −C$\underline{H}_2$−(OC$\underline{H}_2$C$\underline{H}_2$)$_2$−), 5.23 and 5.9 (m, 3H, C$\underline{H}_2$=C$\underline{H}$−), 6.9–8.15 (6d, 12 aromatic protons). ^{19}F NMR: − 243.42 (−CH$\underline{F}$−).
MD312Fs	− 8.647	^{1}H NMR: 0.99 (t, 3H, C$\underline{H}_3$CH$_2$−), 1.12 (d, 3H, −CH(C$\underline{H}_3$)−), 1.44 and 1.67 (m, 2H, CH$_3$C$\underline{H}_2$−), 2.19 (m, 1H, −C$\underline{H}$(CH$_3$)−), 4.93 (dd, 1H, −C$\underline{H}$F−), 3.58–4.22 (m, 14H, −C$\underline{H}_2$−(OC$\underline{H}_2$C$\underline{H}_2$)$_3$−), 5.23 and 5.9 (m, 3H, C$\underline{H}_2$=C$\underline{H}$−), 6.9–8.15 (6d, 12 aromatic protons). ^{19}F NMR: − 243.42 (−CH$\underline{F}$−).
MD312Fr	− 6.17	^{1}H NMR: 0.99 (t, 3H, C$\underline{H}_3$CH$_2$−), 1.09 (d, 3H, −CH(C$\underline{H}_3$)−), 1.44 and 1.63 (m, 2H, CH$_3$C$\underline{H}_2$−), 2.20 (m, 1H, −C$\underline{H}$(CH$_3$)−), 5.05 (dd, 1H, −C$\underline{H}$F−), 3.58–4.22 (m, 14H, −C$\underline{H}_2$−(OC$\underline{H}_2$C$\underline{H}_2$)$_3$−), 5.23 and 5.9 (m, 3H, C$\underline{H}_2$=C$\underline{H}$−), 6.98–8.15 (6d, 12 aromatic protons). ^{19}F NMR: − 251.26 (−CH$\underline{F}$−).
MD112Bs	− 10.042	^{1}H NMR: 0.95 (t, 3H, −CH$_2$C$\underline{H}_3$), 1.12 (d, 3H, −C$\underline{H}$CH$_3$−), 1.38 and 1.68 (m, 2H, −C$\underline{H}_2$CH$_3$), 2.18 (m, 1H, −C$\underline{H}$CH$_3$), 4.21 (dd, 1H, −C$\underline{H}$Br−), 3.81–4.20 (m, 6H, −C$\underline{H}_2$−(OC$\underline{H}_2$C$\underline{H}_2$)−), 5.23 and 5.9 (m, 3H, C$\underline{H}_2$=C$\underline{H}$−), 6.9–8.16 (6d, 14 aromatic protons).
MD212Bs	− 15.187	^{1}H NMR: 0.95 (t, 3H, −CH$_2$C$\underline{H}_3$), 1.12 (d, 3H, −C$\underline{H}$CH$_3$−), 1.38 and 1.68 (m, 2H, −C$\underline{H}_2$CH$_3$), 2.18 (m, 1H, −C$\underline{H}$CH$_3$), 4.21 (dd, 1H, −C$\underline{H}$Br−), 3.81–4.32 (m, 10H, −C$\underline{H}_2$−(OC$\underline{H}_2$C$\underline{H}_2$)$_2$−), 5.23 and 5.9 (m, 3H, C$\underline{H}_2$=C$\underline{H}$−), 6.9–8.16 (6d, 12 aromatic protons).
MD312Bs	− 7.338	^{1}H NMR: 0.95 (t, 3H, −CH$_2$C$\underline{H}_3$), 1.12 (d, 3H, −C$\underline{H}$CH$_3$−), 1.38 and 1.68 (m, 2H, −C$\underline{H}_2$CH$_3$), 2.18 (m, 1H, −C$\underline{H}$CH$_3$), 4.21 (dd, 1H, −C$\underline{H}$Br−), 3.81–4.31 (m, 14H, −C$\underline{H}_2$−(OC$\underline{H}_2$C$\underline{H}_2$)$_3$−), 5.23 and 5.9 (m, 3H, C$\underline{H}_2$=C$\underline{H}$−), 6.9–8.16 (6d, 12 aromatic protons).

[a] These values were measured in CHCl$_3$ at 25°C.
[b] These values were measured in CDCl$_3$, using 400 MHz NMR spectroscopy (internal standard tetramethylsilane).

MD312Fr stands for the following compound: 4′-[(2*R*,3*S*)-2-fluoro-3-methylpentanoyloxy]-4-biphenyl 4-{2-[2-(2-allyloxyethoxy)ethoxy]ethoxy}benzoate (MD312Fr).

MDn12Bs stands for the following series: 4′-[(2*S*,3*S*)-2-bromo-3-methylpentanoyloxy]-4-biphenyl 4-(2-allyl-oxy-ethoxy)benzoate (MD112Bs); 4′-[(2*S*,3*S*)-2-bromo-3-methylpentanoyloxy]-4-biphenyl 4-[2-(2-allyl-oxy-ethoxy)ethoxy]benzoate (MD212Bs); 4′-[(2*S*,3*S*)-2-bromo-3-methylpentanoyloxy[-4-biphenyl 4-{2-[2-(2-allyl-oxy-ethoxy)ethoxy]ethoxy}benzoate (MD312Bs).

2.4. *Synthesis of FLCPs, PS312Fr, PS312Fs, PS312C and PS312Bs*

The structures of the synthesized liquid crystalline polysiloxanes are shown in scheme 4. They were synthesized by similar methods; as an example, the procedure for PS312Bs is described below.

FLC monomer, MD312Bs (0.5 g, 10 mol % excess versus the Si–H groups present in the polysiloxane), was dissolved in 50 ml of freshly distilled toluene together with the appropriate amount of poly(methylhydrogensiloxane). This solution was heated to reflux under N_2. Hydrogen hexachloroplatinate(IV) hydrate (100 µg) in dry THF was then injected via a syringe, and the solution heated at reflux under N_2 for 24 h. After this reaction time, ^{1}H NMR analysis indicated that the hydrosilation reaction was completed. The solution was evaporated under reduced pressure to give crude yellow powder; this product was further purified by precipitation with methanol, and dried under vacuum.

3. Results and discussion
3.1. *Synthesis*

The synthetic routes for FLCs and FLCPs are outlined in schemes 1–4. Chemical structures of the compounds were identified by ^{1}H NMR and ^{19}F NMR. In the ^{1}H NMR spectra, the chemical shift appearing at 4.9 ppm can be associated with the −C<u>H</u>F− proton of the chiral centre of MD*n*12Fs. The peak appearing at 5.1 ppm can be assigned to the −C<u>H</u>F− proton of the chiral centre of MD312Fr. The peak appearing at 4.21 ppm can be assigned to the −C<u>H</u>Br− proton of the

chiral centre of MD*n*12Bs. The chemical structures of compounds MD*n*12Fs and MD312Fr were also identified by ^{19}F NMR. In the ^{19}F NMR spectra, the fluorine chemical shifts appeared at −243.49 and −251.24 ppm for MD*n*12Fs and MD312Fr, respectively. Optical rotations, $[\alpha]_D^5$, of these monomers are summarized in table 1.

The FLCPs were synthesized by hydrosilation reactions in which 10 mol % excess of the LFC monomers was employed to react with the Si–H groups on the poly-(methylhydrogensiloxane) backbone. Chemical structures of the FLCPs were characterized by ^{1}H NMR spectra in which the Si–H peak (4.7 ppm) and vinyl protons of the C<u>H</u>$_2$=C<u>H</u>− group appearing between 5.23 and 5.90 ppm vanished after reaction. This confirmed that complete reaction between FLC monomers and Si–H groups had taken place.

3.2. *Thermal properties*

Phase sequences and their corresponding transition temperatures for compounds MD*n*12Fs, MD312Fr, MD*n*12C, and MD*n*12Bs are shown in table 2.

3.2.1. *MDn12Fs series*

There are three compounds in this series; they consist of the (2*S*,3*S*)-2-fluoro-3-methylpentanoyloxy chiral moiety and an oxyethylene spacer unit. MD112Fs and MD212Fs exhibited similar liquid crystal behaviours with a cholesteric–chiral smectic C–chiral smectic F sequence. No chiral smectic F phase was observed in MD312Fs. The phase assignment was made by POM and XRD. An optical polarized micrograph reveals an oily streak texture at 80°C which corresponds to a cholesteric structure. Figure 1 presents the temperature-dependent XRD diagrams obtained from a powder sample of MD312Fs at 30, 40, 50, 60, and 70°C. Upon further cooling from the cholesteric phase, a sharp low angle reflection (associated with the smectic layer) and a broad wide angle reflection (associated with lateral packings) were observed. Curve A exhibits a diffused reflection at 4.81 Å and a very weak reflection at 28.26 Å, which correspond to smectic layers. Moreover, the *d*-spacing of the first order reflection reduces from 28.36 to 27.26 Å
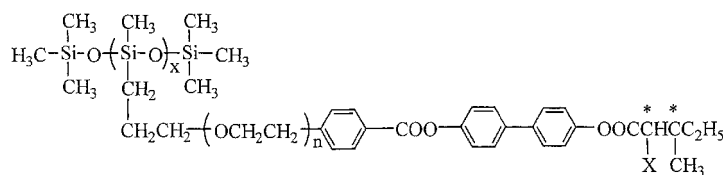
Scheme 4.   The polysiloxane series PS312Fr, PS312Fs, PS312C and PS312Bs.

X=F(R); PS312Fr
X=F(S); PS312Fs
X=Cl(S); PS312C
X=Br(S); PS312Bs

Table 2. Phase transitions and phase transition enthalpies for compounds MD*n*12Fs, MD312Fr, MD*n*12C and MD*n*12Bs: Cr = crystalline phase, SmX = high order smectic phase, SmF* = chiral smectic F phase, SmC* = chiral smectic C phase, Ch = cholesteric phase, I = isotropic phase.

Compound	n^a	$\dfrac{\text{Heating}}{\text{Cooling}}$ Phase transition temperature/°C; (corresponding enthalpy changes/mJ mg^{-1})
MD112Fs	1	Cr 17.6 (0.2) SmX 60.3 (0.1) SmF* 78.3 (1.2) SmC* 126.1 (5.6) Ch 168.5 (0.8) I
		I 166.9 (0.9) Ch 123.9 (5.8) SmC* 76.7 (1.5) SmF* 57.6 (0.1) SmX 17.6(−)^b Cr
MD212Fs	2	Cr 44.6 (18) SmF* 48.2(−) SmC* 100.5 (5.8) Ch 126 (0.6) I
		I 124.6 (0.7) Ch 98.7 (6.1) SmC* 20.8 (0.2) SmF* 8.7 (7.1) Cr
MD312Fs	3	Cr 27.7 (14.6) SmC* 70.6 (5.1) Ch 83.9 (0.4) I
		I 81.3 (0.2) Ch 67.0 (4.9) SmC* 20.8 (0.3) SmX − 6.8 (2.1) Cr
MD312Fr	3	Cr 29.1 (12.9) SmF* 42.9 (0.8) SmC* 82.7 (4.9) Ch 106.9 (5) I
		I 105.5 (0.5) Ch 80.9 (4.8) SmC* 40.2 (0.4) SmX 12.0 (10.5) Cr
MD112C	1	Cr 29.9 (7.4 (SmX 57.1 (1.4) SmC* 113.2 (7.2) Ch 141.7 (0.9) I
		I 142.2 BPII 141.8 BPI 136 (1.1) Ch 112.1 (7.3) SmC* 53.9 (1.9) SmF* 23.9 (1.0) Cr
MD212C	2	Cr − 9.2 (4.2) SmC* 88.3 (7.3) Ch 103.5 (0.8) I
		I 102 BPII 96.6 BPI 90.2 (1.8) Ch 85.9 (7.8) SmC* − 13.9 (5.8) Cr
MD312C	3	Cr 25.26(−)^b SmC* 57.59 (5.3) BP 63.5 (0.2) I
		I 63.77 (0.3) BP 58.6 (5.3) SmC* − 28.13(−)^b Cr
MD112Bs	1	Cr 28.6 (8.9) SmF* 67.6 (33.3) SmC* 104.7 (5.8) Ch 138.2 (0.7) I
		I 136.9 (0.6) Ch 102.9 (5.9) SmC* 54.6 (0.6) SmF* 23.7 (3.2) Cr
MD212Bs	2	Cr − 10.0 (2.1) SmF* 25(−)^b SmC* 81.3 (5.3) Ch 101.15 (0.8) I
		I 99.2 (0.6) Ch 77.7 (5.6) SmC* 23.1 (0.3) SmF* − 13.6 (0.5) Cr
MD312Bs	3	Cr− 25.4 (0.2) SmC* 53.85 (4.2) Ch 65.31 (0.4) I
		I 63.84 (0.4) Ch 51.31 (4.2) SmC* − 28.6 Cr

^{a} *n* corresponds to spacer length.
^{b} Enthalpies were too small to be evaluated.

(curve A to curve E) as the temperature of measurement decreases from 70 to 30°C. The temperature dependence of the layer spacing for MD*n*12Fs is presented in figure 2. In one example, the optical polarizing micrograph of MD312Fs reveals a striated fan texture (figure 3) from 27.7 to 70.6°C. These results imply the presence of a tilted SmC* phase. In figure 4, the tilt angle is plotted as a function of temperature in the chiral smectic C phase; it decreased with increasing temperature. The tilt angles were calculated from equation (1); $d_{\text{SmC}^*\text{(Max)}}$ was chosen to be the maximum layer spacing of the chiral smectic C phase.

$$\theta = \cos^{-1}\left(\frac{d_{\text{SmC}^*}}{d_{\text{SmC}^*\text{(Max)}}}\right). \qquad (1)$$

The temperature angle of the chiral smectic phase was about 50°C. From figure 5, it can be seen that the increasing number of oxyethylene units significantly depresses the phase transition temperature [15]. This depression has been attributed to the increased flexibility of the C–O bonds.

3.2.2. *MD312Fr*

This compound contained the (2*R*,3*S*)-2-fluoro-3-methylpentanoyloxy chiral moiety and three oxyethylene spacer units. A cholesteric–chiral smectic C–chiral smectic F liquid crystal sequence was found. Upon cooling from the cholesteric phase, the chiral smectic C phase, and chiral smectic F with striated fan textures were formed. The (2*R*,3*S*)-2-fluoro-3-methylpentanoyloxy chiral moiety showed a poorer mesomorphic behaviour as compared with MD312Fs.

3.2.3. *MDn12C series*

The MD*n*12C series contained the (2*S*,3*S*)-2-chloro-3-methylpentanoyloxy chiral moiety and oxyethylene spacer units (*n* = 1–3) [14]. The three compounds in this series are all mesomorphic; all three compounds display the chiral smectic C phase. The mesophase ranges of MD*n*12C and MD*n*12Fs are shown in table 2. A wider chiral smectic C phase and lower clearing temperature for MD*n*12C were observed. MD112Fs and MD212Fs are more inclined to form the ordered
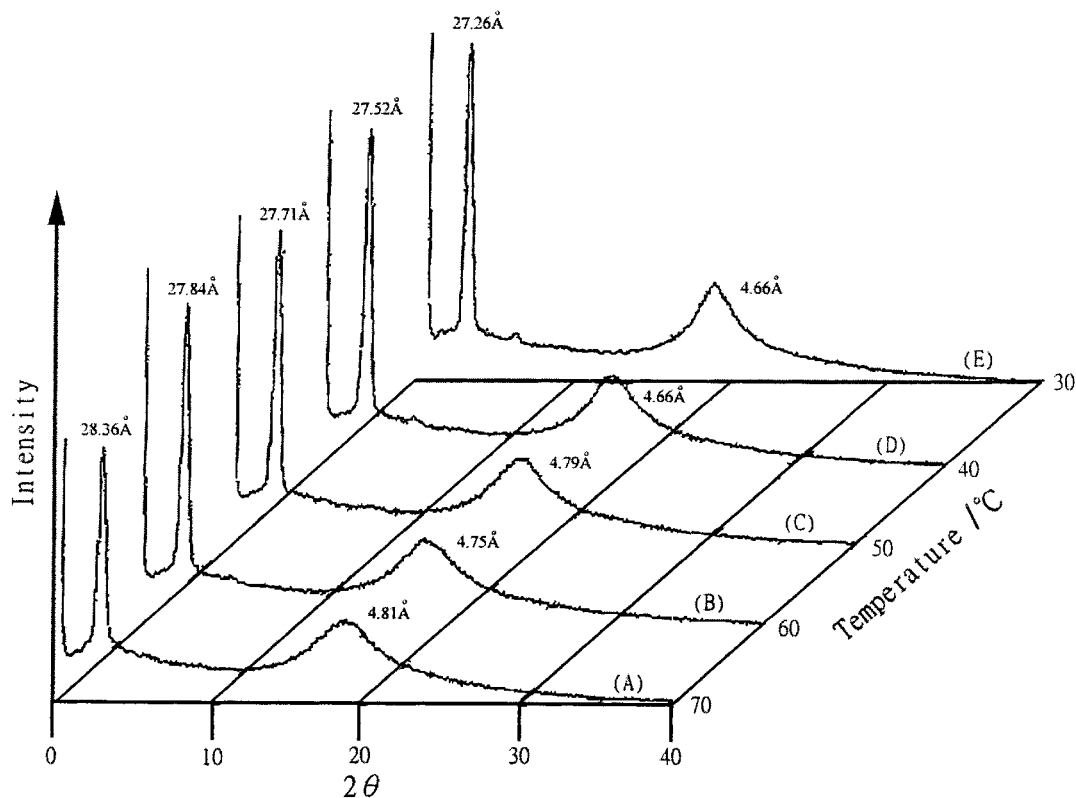
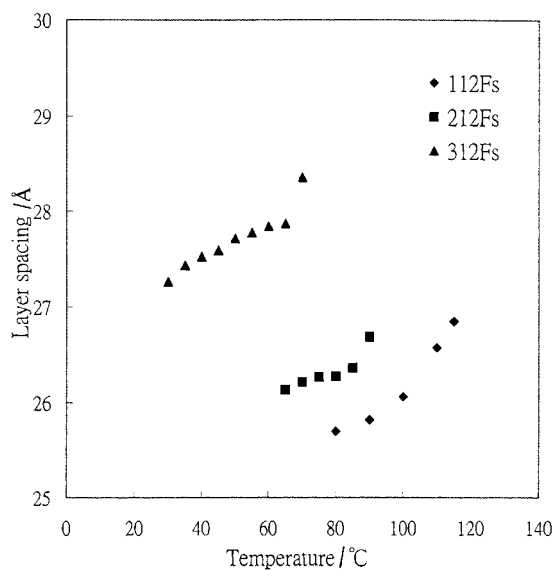Figure 1.   X-ray diffraction measurements for MD312Fs.

Figure 2.   Layer spacing as a function of temperature in the chiral smectic C phase of compounds MD*n*12Fs.

Figure 3.   Optical polarizing micrograph of MD312Fs showing the chiral smectic C phase at 50°C (400 ×).

chiral smectic F phase as compared with MD112C and MD212C. This implies that the decreasing dipole moment and increasing atomic size of the halogen in the chiral moiety can decrease the clearing temperature and widen the chiral smectic C phase.
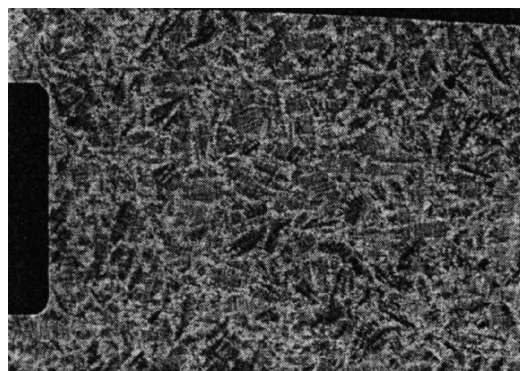
3.2.4. *MDn12Bs series*

The MD*n*12Bs series contained the (2*S*,3*S*)-2-bromo-3-methylpentanoyloxy chiral moiety and oxyethylene spacer units ($n = 1$–3). MD112Bs and MD212Bs exhibited similar liquid crystal behaviours with a cholesteric–chiral smectic C–chiral smectic F liquid crystal sequence. The chiral smectic F phase was not observed for the compound with longest spacer length, MD312Bs. XRD measurements and POM verified the assignment of the mesophases for these compounds. For compounds MD*n*12Bs, a sharp low angle reflection and a broad wide
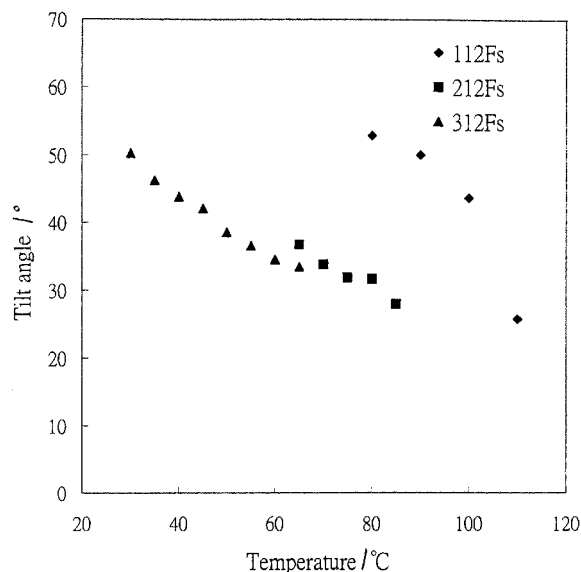
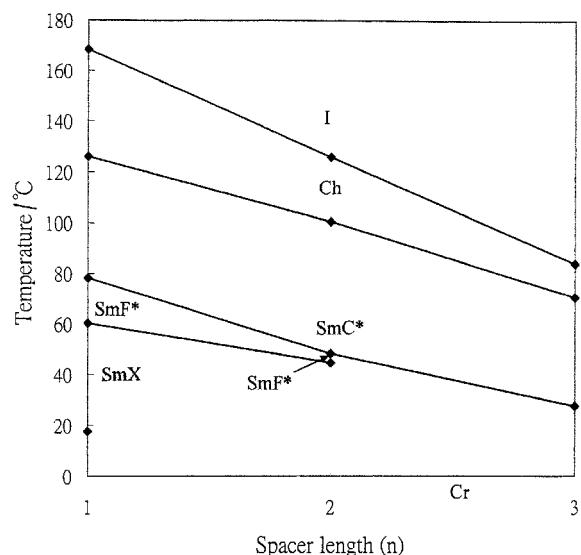Figure 4. Tilt angles as a function of temperature in the chiral smectic C phase of compounds MD*n*12Fs.

Figure 5. Plots of transition temperature versus *n*, the number of oxyethylene spacer units for compounds MD*n*12Fs.

Figure 6. Optical polarizing micrograph of MD112Bs showing the chiral smectic C phase at 75°C (400×).

Figure 7. Plots of transition temperature versus *n*, the number of oxyethylene spacer units for compounds MD*n*12Bs.

angle reflection angle were observed in XRD diagrams; these were respectively assigned to lateral packing and the smectic layer below the cholesteric point. Moreover, the tilt angle decreases as the temperature increases. In one example, the optical polarizing micrograph reveals a striated fan texture (figure 6) from 67.6 to 104.7°C for MD112Bs. This indicates the formation of the tilted chiral smectic C phase. The temperature range of the chiral smectic phase was about 80°C for MD312Bs. The clearing temperature and phase transition temperature decreased as the number of oxyethylene units increased (figure 7). Moreover, the clearing point of the MD*n*12Fs
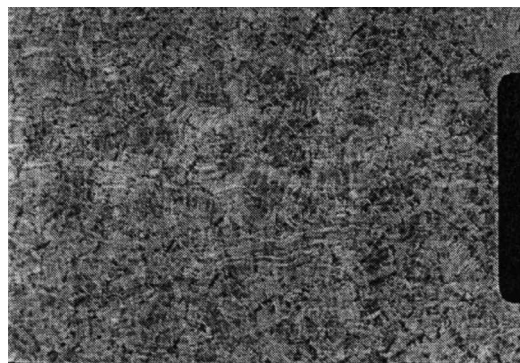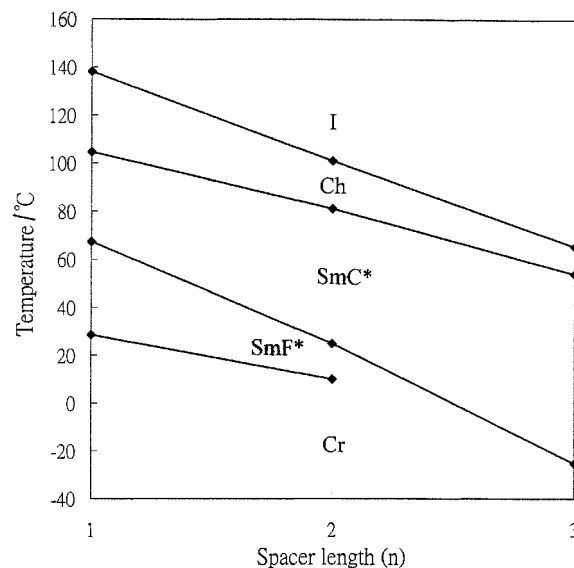
series is higher than for the MD*n*12Bs series. This may result from the increase in dipole moment and decrease in molecular size of the asymmetric chiral center [16].

3.2.5. *Polymer series PS312Fr, PS312Fs, PS312C and PS312Bs*

The phase sequences and corresponding transition temperatures for the (*n* = 3) members of these series are shown in table 3. Polymers PS312Fs, PS312Fr, and PS312C exhibited similar liquid crystal behaviour, with cholesteric and chiral smectic C phases on the heating and cooling scans. XRD measurement for PS312Fs and PS312Fr show a smectic diffraction pattern (a sharp low angle reflection and a broad wide angle reflection). Layer spacings were plotted as a function of temperature in the chiral smectic C phase (figure 8); the layer spacing increases as the temperature increases, confirming the presence of the chiral smectic C phase. On the other

Table 3. Phase transitions and phase transition enthalpies for polymers PS312Fs, PS312Fr, PS312C, and PS312Bs: g = glassy state, SmF* = chiral smectic F phase, SmC* = chiral smectic C phase, Ch = cholesteric phase, I = isotropic phase.

Polymer	n^a	Heating / Cooling Phase transition temperature/°C; (corresponding enthalpy changes/mJ mg^{-1})
PS312Fr	3	g 25.9 SmC* 139.4 Ch 160.5 I
		I 150.5 Ch 131.4 SmC* 24.4 g
PS312Fs	3	g 28.6 SmC* 143 Ch 163 I
		I 153.34 Ch 137.4 SmC* 32.4 g
PS312C	3	g 17 SmC* 131.9 Ch 149.8 I
		I 145.5 Ch 128.1 SmC* 12 g
PS312Bs	3	—
		I 105.4 (0.6) Ch 7.4 (0.7) g

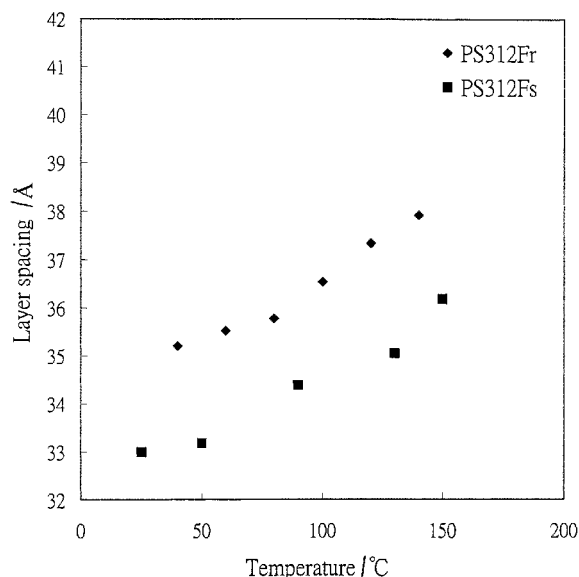^{a} *n* corresponds to spacer length.

Figure 8. Layer spacing as a function of temperature in the chiral smectic C phase of polymers PS312Fs and PS312Fr.

hand, PS312Fs, PS312Fr, and PS312C reveal wider temperature ranges of the SmC* phase as compared with MD312Fr, MD312Fs, and MD312C. For PS312C, the temperature range of the chiral smectic C phase was about 120°C. A flexible polysiloxane backbone enhances the decoupling between side chain and main chain, tending to give rise to a higher thermal stability of the mesophases, including the chiral smectic C phase [17]. Sample PS312Bs exhibited fewer mesomorphic phases and no chiral smectic C phase. This may result from the

more bulky molecular size of asymmetric chiral centre [16], which reduces the phase stability of ferroelectric liquid crystal homopolymer.

4. Conclusion

A new series of ferroelectric liquid crystal monomers and polymers consisting of a halogenated chiral centre, oligooxyethylene spacers, and an ester core unit containing three aromatic rings have been synthesized. All of the compounds exhibit the chiral smectic C phase except PS312Bs. Wide SmC* temperature ranges were obtained in these monomers (~90°C) and polymers (~100°C). Several MDn12Fs, MDn12Fr, and MDn12Bs compounds (n = 1, 2) exhibited chiral smectic F phases. When the number of oxyethylene spacer units increased, the clearing and phase transition temperatures decreased. The lack of mesophases in PS312Bs is possibly due to the bulky substituted group at the chiral centre which disturbs the orientation of the side chain liquid crystal polymer.

References

[1] MEYER, R. B., LIEBERT, L., STRZELECKI, L., and KELLER, P., 1975, *J. Phys. Paris Lett.*, **36,** L-69.
[2] CLARK, N. A., and LAGERWALL, S. T., 1980, *Appl. Phys. Lett.*, **36,** 899.
[3] ZENTAL, R., RECKERT, G., and RECK, B., 1987, *Liq. Cryst.*, **2,** 83.
[4] PARMAR, D. S., CLARK, N. A., KELLER, P., WALBA, D. M., and WAND, M. D., 1990, *J. Phys. Paris.*, **51,** 355.
[5] DUMON, M., NGUYEN, H. T., MAUZAC, M., DESTRADE, C., and GASPAROUX, H., 1991, *Liq. Cryst.*, **10,** 475.
[6] NACIRI, J., PFEIFFER, S., and SHASHIDHAR, 1991, *Liq. Cryst.*, **10,** 585.
[7] LU, R., XU, K., and LU, Z., 1999, *Liq. Cryst.*, **26,** 553.
[8] KELLER, P., 1984, *Mol. Cryst. liq. Cryst.*, **102,** 295.
[9] ADAMS, T. G., and SINTA, R., 1989, *Mol. Cryst. liq. Cryst.*, **177,** 145.
[10] COLLINGS, P. J., and HIRD, M., 1997, *Introduction to Liquid Crystals* (London: Taylor & Francis Ltd), p. 51.
[11] CHEN, J. H., CHANG, R. C., HSIUE, G. H., GUU, F. W., and WU, S. L., 1995, *Liq. Cryst.*, **18,** 291.
[12] SIERRA, T., SERRANO, J. L., ROS, M. B., EZURRA, A., and ZUBIA, J., 1992, *J. Am. chem. Soc.*, **114,** 7645.
[13] COLLINGS, P. J., and HIRD, M., 1997, *Introduction to Liquid Crystals* (London: Taylor & Francis Ltd), p. 119.
[14] HSIUE, G. H., WU, J. L., and CHEN, J. H., 1996, *Liq. Cryst.*, **21,** 449.
[15] KITAMURA, T., FUJII, T., and MUKOH, A., 1984, *Mol. Cryst. liq. Cryst.*, **108,** 333.
[16] COLLINGS, P. J., and HIRD, M., 1997, *Introduction to Liquid Crystals* (London: Taylor & Francis Ltd), p. 120.
[17] HSIUE, G. H., and CHEN, J. H., 1995, *Macromolecules*, **28,** 4366.